

Research article

**PROTEOMIC ANALYSIS OF TUMOR TISSUE IN CT-26 IMPLANTED
BALB/C MOUSE AFTER TREATMENT WITH ASCORBIC ACID**JIHYE LEE¹, GUNSUP LEE², JIN HEE PARK², SUKCHAN LEE²,
CHANG-HWAN YEOM³, BYUNGJO NA⁴ and SEYEON PARK^{1*}Department of Applied Chemistry, Dongduk Women's University,
23-1 Wolgok-dong, Sungbuk-ku, Seoul 136-714, Korea, ²Department of Genetic
Engineering, Sungkyunkwan University, Suwon, Korea, ³Yeom's Clinic
of Palliative Medicine, Seoul, Korea, ⁴Weedam Korean Hospital, Seoul, Korea

Abstract: Tumor establishment and penetration consists of a series of complex processes involving multiple changes in gene expression and protein modification. Proteome changes of tumor tissue were investigated after intraperitoneal administration of a high concentration of ascorbic acid in BALB/C mice implanted with CT-26 cancer cells using two-dimensional gel electrophoresis and mass spectrometry. Eighteen protein spots were identified whose expression was different between control and ascorbic acid treatment groups. In particular, eukaryotic translation initiation factor 3 subunit 1, nucleophosmin, latexin, actin-related protein 2/3 complex subunit 5, M2-type pyruvate kinase, vimentin, tumor protein translationally-controlled 1, RAS oncogene family Ran, plastin 3 precursor, ATPase, Rho GDT dissociation inhibitor β , and proteasome activator subunit 2 expression were quantitatively up-regulated. The increase in the level of these proteins was accompanied by an increase in mRNA level. The cytoskeleton protein actin, vimentin, and tumor protein translationally-controlled 1 showed quantitative expression profile differences. A change in actin cytoskeleton distribution, functionally relevant to the proteome result, was observed after treatment with ascorbic acid. These

* Author for correspondence. e-mail: sypark21@dongduk.ac.kr, phone: +82-2-940-4514, fax: +82-2-940-4193

Abbreviations used: ATP – adenosine triphosphate; DTT – dithiothreitol; ECM – extracellular matrix; GDT – guanosine diphosphate; LR – log ratio; MALDI TOF-MS/MS – Matrix-assisted laser-desorption ionization time-of-flight tandem mass spectroscopy; MMPs – matrix metalloproteinases; PAGE – polyacrylamide gel electrophoresis; PBS – phosphate buffered solution; PCR – polymerase chain reaction; SDS – sodium dodecyl sulfate; TCA – trichloroacetic acid; TCTP – translationally controlled tumor protein; 2-DE – two-dimensional gel electrophoresis

results suggest a previously undefined role of ascorbic acid in the regulation of cytoskeleton remodeling in tumor tissues.

Key words: Cytoskeleton remodelling, Ascorbic acid, Proteomics, Tumor tissue, mRNA

INTRODUCTION

Ascorbic acid (also termed ascorbate) is toxic to cancer cells when given intravenously at high concentrations [1]. Increasing evidence also indicates that ascorbic acid is selectively toxic to some types of tumor cells as a pro-oxidant, rather than as an anti-oxidant [2, 3]. At concentrations of 10 nM–1 mM, ascorbic acid induces apoptosis in neuroblastoma and melanoma cells [4, 5]. Furthermore, ascorbic acid modulates mouse myeloma cell growth *in vitro*, as well as modulating leukemic progenitor cell growth in cells from patients with acute myeloid leukemia and myelodysplastic syndrome [6-8].

The common characteristics of cancer cells are invasiveness and metastasis, both of which play important roles in secondary tumor development and progression, and which influence patient mortality. Attachment and penetration of cancer cells affects the extent of invasion and metastasis [9]. Cancer cells form tumors that can spread by degrading the extracellular matrix (ECM) through various matrix metalloproteinases (MMPs) [10]. Nutrients such as lysine and ascorbic acid are postulated to act as natural inhibitors of ECM proteolysis, and as such have the potential to inhibit tumor growth and expansion [11]. These nutrients may exert their antitumor effects via inhibition of MMPs and strengthening the connective tissue surrounding cancer cells. Additionally, it has been suggested that, through inhibition of hyaluronidase, ascorbic acid can prevent metastases by preventing degradation of the ground substance surrounding the tumor [12]. Different mechanisms are involved in the metastatic cascade including angiogenesis, cellular adhesion, local proteolysis, and tumor cell migration [9, 13]. Tumor development and progression consist of a series of complex processes involving multiple changes in gene expression [10].

Time-lapse analyses of Walker 256 carcinosarcoma cell migration showed that both the speed of movement and cell displacement are inhibited by ascorbic acid [14]. These results demonstrate that intact, unmodified ascorbic acid applied in physiologically relevant and nontoxic concentrations exerts an inhibitory effect on the migration of WC 256 carcinosarcoma cells, and that this may be one of the factors responsible for the anti-metastatic activity of ascorbic acid. Additionally, sodium ascorbate supplementation of drinking water inhibits subcutaneous tumor growth, enhanced levodopa methyl ester chemotherapy, and increased survival of B 16 melanoma-bearing mice [15]. Spontaneous metastasis was found to be inhibited by ascorbate in mice fed the restricted diet [15]. Recently, the ability of orally administered vitamins C and K3 to inhibit the development of metastases of mouse liver tumor (TLT) cells that have been

implanted into the thigh of C3H mice was evaluated [16]. Similar experiments, using ascorbate and menadione with human prostate carcinoma, have shown that tumor cells reactivate nucleases to affect their morphology via the cytoskeleton and die by a new cell death, called autschizis, as shown by Taper et al. [17].

To understand the molecular basis of ascorbic acid's effect on tumor formation, we investigated the proteins whose expression was altered in the presence of ascorbic acid. In the present study, we performed two-dimensional gel electrophoresis (2-DE) using tumor nodules of mice implanted with CT-26 cancer cells following the administration of a high dose of ascorbic acid.

MATERIALS AND METHODS

Mice groups

Six-week-old BALB/C mice purchased from Dae Han BioLink (Seoul, Korea) were fed a basal diet for experimental animals. The mice were assigned to one of two groups (each group consisted of five mice) based on the ascorbic acid administration regimen applied. One group consisted of controls that lacked ascorbic acid. Two groups were injected with tumor cells, with subsequent injection of normal saline (control group) or ascorbic acid (treatment group). Principles of laboratory animal care (NIH publication 85-23, revised 1986) were followed and all experiments were carried out with Association for Assessment and Accreditation of Laboratory Animal Care International approval.

Implantation of cancer cells and assessment of tumor formation

Viable neoplastic CT-26 murine colon adenocarcinoma cells (10^6) were implanted in mice via intraperitoneal injection. The cells were cultured *in vitro* in RPMI 1640 medium (Gibco, Grand Island, NY) supplemented with 10% heat-inactivated fetal bovine serum (Hyclone, Salt Lake City), 100 IU/ml penicillin, and 100 μ g/ml streptomycin. The cells were subcultured at a split ratio (1:4) for injection; > 95% of the total cells were viable as determined by the exclusion of trypan blue. Mice in the treatment group were intraperitoneally injected with ascorbate (1.5 mg/g body weight) every three days. The injections were performed by Huons Co. (Seoul, Korea). All mice were sacrificed by general anesthesia 30 days after tumor transplantation. After sacrifice, a detailed general autopsy of each mouse was performed to identify tumor nodule formation.

Preparation of total protein extracts for two dimensional gel electrophoresis

To obtain total protein extracts, the tumor nodule was washed and homogenized in 2-DE sample buffer containing 7 M urea, 2 M thiourea, 4% (w/v) CHAPS, 100 mM dithiothreitol (DTT), and a protease inhibitor cocktail (Roche, Basel, Switzerland). Tissue was disrupted by several strokes with a sonicator. After 30 min of incubation with DNase (100 U/ml) at 4°C, tissue lysates were centrifuged at 45 000 rpm for 45 min at 4°C. The supernatant was collected in a new tube.

Precipitation using trichloroacetic acid (TCA; Sigma-Aldrich, St. Louis, MO) and acetone was performed to purify the protein. TCA (50% v/v) was added to produce a final concentration of 5%-8%. The sample was mixed by inversion and incubated on ice for 2 h. Following centrifugation at 14 000 rpm for 20 min, the supernatant was discarded and the protein pellet was resuspended in 200 μ l of cold acetone. After incubation on ice for 15 min, the sample was centrifuged at 14 000 rpm for 20 min and dried. The dried pellet was dissolved in 2-DE sample buffer and the protein concentration was determined using a Bradford protein assay kit (Bio-Rad, Hercules, CA).

Two dimensional gel electrophoresis

Protein (800 μ g) was diluted to a final volume of 300 μ l in sample buffer containing 7 M urea, 2 M thiourea, 4% (w/v) CHAPS, 100 mM DTT, and 0.5% carrier ampholyte (pH 4-7, Bio-Rad) and loaded on a 17 cm long gel with pH 4-7 gradient. A rehydrated immobilized pH gradient (IPG) strip was positioned gel side down on the strip tray and covered with mineral oil. The voltage was sequentially increased from 100 V to 8000 V to attain 80 000 total volt-hours (300 Vh at 100 V, 400 Vh at 200 V, 1000 Vh at 500 V, 1000 Vh at 1000 V, 2000 Vh at 2000 V, 4000 Vh at 4000 V, for a total of 80 000 Vh at 8000 V). During IEF, the temperature was set to 20°C. To solubilize the focused proteins, the IPGs were soaked in sodium dodecyl sulfate (SDS) equilibration buffer containing 6 M urea, 2% (w/v) SDS, 0.05 M Tris-HCl (pH 8.8), and 20% glycerol. The strip was treated with 10 ml of an equilibration solution containing 6 M urea, 2% (w/v) SDS, 0.05 M Tris-HCl (pH 8.8), 20% glycerol, and 20% DTT, and placed on a shaker for 10 min. Then the strip was shaken in 10 ml of iodoacetamide equilibration solution containing 6 M urea, 2% (w/v) SDS, 0.05 M Tris-HCl (pH 8.8), 20% glycerol, and 25% IAA for another 10 min. After briefly rinsing with 1x gel buffer, the IPG strip was loaded on the top of 12% SDS-polyacrylamide gel electrophoresis (PAGE) gel. Low melting point agarose consisting of 1% molten agarose solution with a trace amount of bromophenol blue was added. SDS-PAGE was performed for 30 min at a constant current of 16 mA and then at 24 mA at 4°C.

Two dimensional gel image analysis

Electrophoretically separated proteins were visualized by Coomassie brilliant blue G-250 staining of the gels. Images were digitalized using a GS-800 calibrated densitometer (Bio-Rad) and analyzed by PD Quest 2-D software (Bio-Rad). Quantitative differences were determined only when a matched spot displayed the same degree of down- or up-regulation in duplicate experiments. Matching spots in gels from the same sample were identified and their intensities were measured using an Image Master 2-D system. Analysis was performed on approximately 170 different protein spots per sample. For each spot, the intensity value obtained in the ascorbic acid-treated gel was divided by that obtained in the control gel. The logs of these ratios (LR; the means and median

values clustered around the 0 value) were then calculated. The LR was expected if errors associated with the analysis were random and normally distributed. Spots showing an expression 3.0-fold less or greater than the control were considered to represent a statistically significant differentially expressed protein species.

In-gel enzymatic digestion and mass spectrometry

Spots were excised from the stained gel, destained with 50 mM ammonium bicarbonate in 40% acetonitrile, and dried with a Speed Vac plus SC1 10 (Savant Holbrook, HY). The excised spot was rehydrated in 10 ng/ μ l trypsin in 50 mM ammonium bicarbonate. After the rehydrated spot was placed on ice for 45 min and treated with 50 mM ammonium bicarbonate (10 μ l), it was incubated at 37°C for 12 h.

Matrix-assisted laser-desorption ionization time-of-flight tandem mass spectrometry (MALDI TOF-MS/MS)

Digested samples were removed and subjected to a desalting/concentration step on a mZipTipC18 column (Millipore, Billerica, MA) using acetonitrile as an eluent before MALDI-TOF-MS/MS analysis. Peptide mixtures were loaded on the MALDI system using the dried-droplet technique and α -cyano-4-hydroxycinnamic acid (Sigma) as matrix, and were analyzed using a 4700 Reflector spec #1 mass spectrometer (Applied Biosystems, Framingham, MA). Internal mass calibration was performed using peptides derived from enzyme autolysis. The Data Explorer software package (Applied Biosystems) was used to identify spots from the ProFound database by mass searching all taxa sequences. Candidates identified by peptide mapping analysis were evaluated further by comparing their calculated masses and isoelectric points using the experimental values obtained by 2-DE.

Immunohistochemistry

Tumor nodules were fixed in 10% neutral formalin, embedded in paraffin, cut into 4 μ m thick sections using a microtome (Probe-On-Plus Slides, Fisher Scientific, Waltham, MA), and dried. Paraffin sections were deparaffinized in xylene and rehydrated in ethanol and water. The sections were incubated for 30 minutes in 0.3% H₂O₂, thus avoiding endogenous peroxidase activity. After washing with phosphate buffered solution (PBS), the sections were incubated in 0.01 M sodium citrate (pH 6.0) for 10 minutes at 95°C and cooled to room temperature. In order to avoid the background activity, sections were incubated in 4% bovine serum albumin with dextran for 20 minutes. The sections were incubated with several primary antibodies for 1 h according to their own protocols. After applying the mouse anti-beta actin primary monoclonal antibodies (Abcam, Cambridge, MA), the sections were incubated with mouse secondary antibody (DAKO, Berkshire, UK) for 30 minutes at room temperature. The sections were then washed in PBS, stained with diaminobenzidine tetrahydrochloride solution (DAKO), and counter-stained with hematoxylin (Sigma) [18-23]. The sections were analyzed using an Olympus BX 40 light microscope.

RNA isolation and polymerase chain reaction (PCR)

For the validation of the 2-DE proteomics data, real-time PCR was performed. Total RNA was extracted by homogenization in Trizol reagent (Invitrogen, Carlsbad, CA) according to the manufacturer's instructions from the isolated tumor tissue of each mouse. Synthesis of cDNA was performed as previously described [24]. Briefly, 50 µg of total RNA was reverse-transcribed to double stranded cDNA using an oligo-dT primer. For PCR analysis, primer pairs were designed for each gene. The information for each probe was obtained from the Stanford Online Universal Resource for Clones and ESTs (SOURCE; <http://www.source.stanford.edu>), which compiles information from several publicly accessible databases including UniGene, dbEST, Swiss-Prot, GeneMap99, RHDdb, GeneCards, and LocusLink. Each probe was designed to have a melting temperature of about 60°C. For real-time PCR, 50 ng of cDNA was mixed with 10 µM of each primer in SYBR Green Master Mix (Takara Bio Inc, Shiga, Japan). Real-time PCR was performed in an ABI PRISM 7700 (Applied Biosystems, Foster City, CA). All amplifications were run in triplicate. Intron-specific primers were used to control for genomic contamination. A no-template control was performed for each primer pair. 18S RNA was selected as the endogenous control. The conditions were optimized to show single peaks in the melting curve. ΔC_T was computed by subtracting the C_T (the number of cycles to reach the threshold) for 18S RNA from the C_T value for each gene. The expression level for each gene expressed in units of 18S RNA was then taken as $2^{-\Delta C_T}$. These units were normalized so that the 18S RNA level was 10 000.

PCR primer: eukaryotic translation initiation factor 3 subunit 1 (forward: 5'-TCACCGCCAGGATGAAAC-3', reverse: 5'-CAGAGTACCACACGTTGACGA-3', amplicon size 129 bp); nucleophosmin 1 (forward: 5'-GAAAAAGGCGGT TCTCTTCC-3', reverse: 5'-TTTCCTCCACTGCCAGAGAT-3', amplicon size 111 bp); latexin (forward: 5'-TCAAAGCCTCATGTCTCTGAAG-3', reverse: 5'-TGTGGAGACACATTTCCAAAA-3', amplicon size 75 bp); actin, beta (forward: 5'--3', reverse: 5'--3', amplicon size bp); capping protein (actin filament), gelsolin-like (forward: 5'-GCTGTGTGGCAAATCTACATC-3', reverse: 5'-GATGAAGCCAT CAGCCACTT-3', amplicon size 88 bp); actin-related protein 2/3 complex subunit 5 (forward: 5'-GGTGGACTCGTGCCTACG-3', reverse: 5'-CTGCCTGGCTCTTT GTGTTA-3', amplicon size 89 bp); M2-type pyruvate kinase (forward: 5'-CAAGATCTACGTGGACGATGG-3', reverse: 5'-TTCTTGCTGCCCAAG GAG-3', amplicon size 105 bp); glutamate dehydrogenase 1 (forward: 5'-CTGGATCGCTGACACCTATG-3', reverse: 5'-GGATGCCTCCTTGACTG ATG-3', amplicon size 95 bp); vimentin (forward: 5'-CCTTTTCTTCCC TGAACCTGA-3', reverse: 5'-TGTTCTTTTTGAGTGGGTG TCA-3', amplicon size 74 bp); tumor protein, translationally-controlled 1 (forward: 5'-GGATGG CTTAGAGATGGAG AAA-3', reverse: 5'-TCCCATTTGTCCTAAAGTCCTG-3', amplicon size 109 bp); RAN, member RAS oncogene family (forward: 5'-TTGTGCCTACCTTCATAAACA TTTAGATTG-3', reverse: 5'-ACACAAGGT CTCTCTTAGGTTAAACTAC-3', amplicon size 106 bp); plastin 3 precursor

(forward: 5'-AATACTGATGACCTGTTC AAAGCA-3', reverse: 5'-TGAAAGG TTGATCATTTTGCAG-3', amplicon size 66 bp); ATPase, H⁺ transporting, lysosomal V1 subunit A (forward: 5'-CCATTATCCGGGAGCACAT-3', reverse: 5'-CTCGCCATCTTTCACCTGGAT-3', amplicon size 80 bp); proteasome 28 subunit beta transcript varian 2 (forward: 5'-TCATATCCCTGAGTCAGCTCTTGG-3', reverse: 5'-GTCTGTTTCCATCTCG TCATCCTTG-3', amplicon size 125 bp); Rho, GDP dissociation inhibitor β (forward: 5'-CATACCGGACTGGCATGAG-3', reverse: 5'-CCCTTGGGAGCTTCCTC TAC-3', amplicon size 109 bp).

RESULTS

Influence of ascorbate on tumor nodule size

In mice injected with CT-26 tumor cells, the tumor nodule began to grow and caused ascites. In the independent first experiment, 0.8226 ± 0.2794 g of tumor mass was measured in the control group, and 0.5983 ± 0.1859 g in the treatment group, showing a significant ($p = 0.031$) reduction in the ascorbic acid-treated group as compared with the control group (Fig. 1 and Tab. 1). In the second experiment, 0.8533 ± 0.1168 g of tumor mass was observed in the control group, and 0.7125 ± 0.1682 g in the treatment group. Although the two groups showed slight differences, there was no significance in the second experiment.

Without ascorbic acid



Treated with ascorbic acid



Fig. 1. Tumor nodule formed after treatment of CT-26 cells. The mice were assigned to one of two groups (each group consisted of five mice) based on the ascorbic acid administration regimen applied. One group consisted of controls that lacked ascorbic acid. Two groups were injected with tumor cells, with subsequent injection of normal saline (control group) or ascorbic acid (treatment group). After 30 days of tumor transplantation, a detailed general autopsy of each mouse was performed to identify tumor nodule formation. These data shown are representative of four independent experiments.

Changes in tumor tissue proteome profile after ascorbic acid treatment

To investigate the molecular basis, proteomic differential display analysis for the expression of proteins in the tumor tissue of mice in control and treatment groups was performed by 2-D gel electrophoresis and MALDI-TOF MS/MS. Protein expression was assessed in six samples each from each group obtained on the same schedule under the same conditions. More than 170 protein spots

were visualized on the 2-DE gels, and the differences in spot intensities between control and treatment groups were compared visually and analyzed for each gel.

Tab. 1. Effects of ascorbic acid on average tumor mass in BALB/C mice transplanted with CT-26. In each experiment, each group was composed of five mice. Data represent the mean \pm SD. Asterisk (*) indicates $P < 0.05$ compared to control group (Student's t test).

Group	Control	Treatment
Average tumor mass (g) (Average \pm S.D.)	^a 0.8226 \pm 0.2794*	^b 0.5983 \pm 0.1859*
	^c 0.8533 \pm 0.1168	^d 0.7125 \pm 0.1682

Experiments were performed independently twice. ^a – 5 mice, ^b – 5 mice with six nodules, ^c – 5 mice with six nodules, ^d – 5 mice

Tab. 2. Protein spots altered by the treatment of ascorbic acid. *Up-regulated proteins, **Down-regulated proteins, +Significantly regulated proteins ($P < 0.05$ compared to control group – Student's t test).

Spot No.	Protein description	Measured Mr(KDa)/PI	Intensity variation	MALDI-TOF coverage(%)
0806	Eukaryotic translation initiation factor 3 subunit 1	83.61/5.0	4.09*	45%
1407	Nucleophosmin 1	32.74/4.6	4.40*	37%
4604	Latexin	61.11/5.7	41.51*+	29%
3510	Actin, beta	42.06/5.3	271.3*	34%
7408	Capping protein (actin filament), gelsolin-like	39.04/6.5	0.031**	65%
4511	Actin-related protein 2/3 complex subunit 5	50.44/5.3	32.4*+	19%
4610	M2-type pyruvate kinase	58.47/7.2	4.55*	36%
7612	Glutamate dehydrogenase 1	61.66/8.3	0.045**	24%
2201	Vimentin	51.60/4.6	3.31*	48%
2505	ATP synthase, H ⁺ transporting mitochondrial F1 complex, beta subunit	56.28/5.2	18.4*+	38%
1105	Tumor protein, translationally-controlled 1	19.56/4.8	4.49*	60%
0201	RAN, member RAS oncogene family	24.58/7.0	66.85*+	30%
4713	Plastin 3 precursor	71.24/5.4	13.57*+	22%
4711	ATPase, H ⁺ transporting, lysosomal V1 subunit A	68.65/5.4	15.85*	20%
4308	Proteasome activator subunit 2 isoform 1	27.27/5.5	56.56*+	32%
7421	Rho, GDP dissociation inhibitor β	36.75/6.7	17.30*+	41%
8310	Glyceraldehyde-3-phosphate dehydrogenase	36.08/8.7	66.1*+	32%
5505	Alpha-enolase (2-phospho-D-glycerate hydro-lyase) (Non-neural enolase) (NNE) (Enolase 1)	47.47/6.4	11.9*	26%

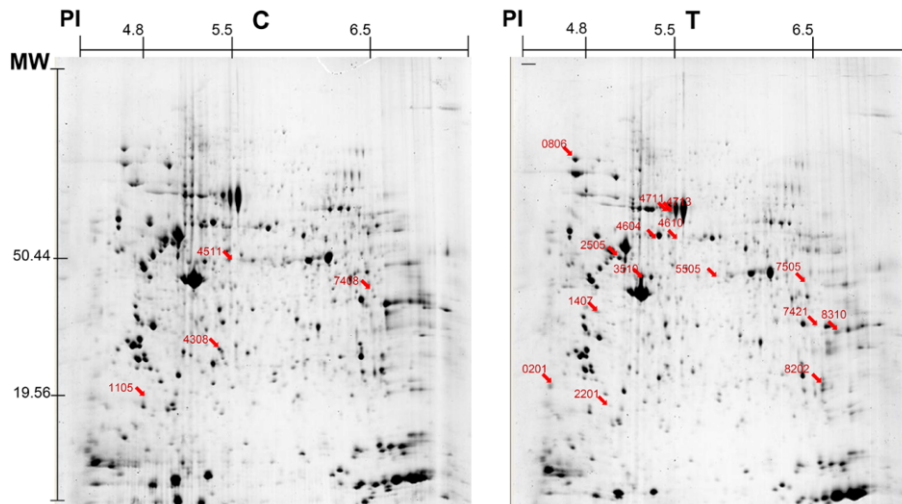


Fig. 2. Examination of tumor nodule proteins by 2-DE. Results shown are representative of four independent experiments. The images were analyzed by ImageMaster 2D software and proteins were identified by MALDI-TOF MS/MS. Total protein extracts were analyzed by 2DE and gels were stained with Coomassie brilliant blue G-250. Vertical axes represent apparent molecular mass (kDa) and horizontal axes pH values. Acquired images of four independent experiments showed a repetitive pattern.

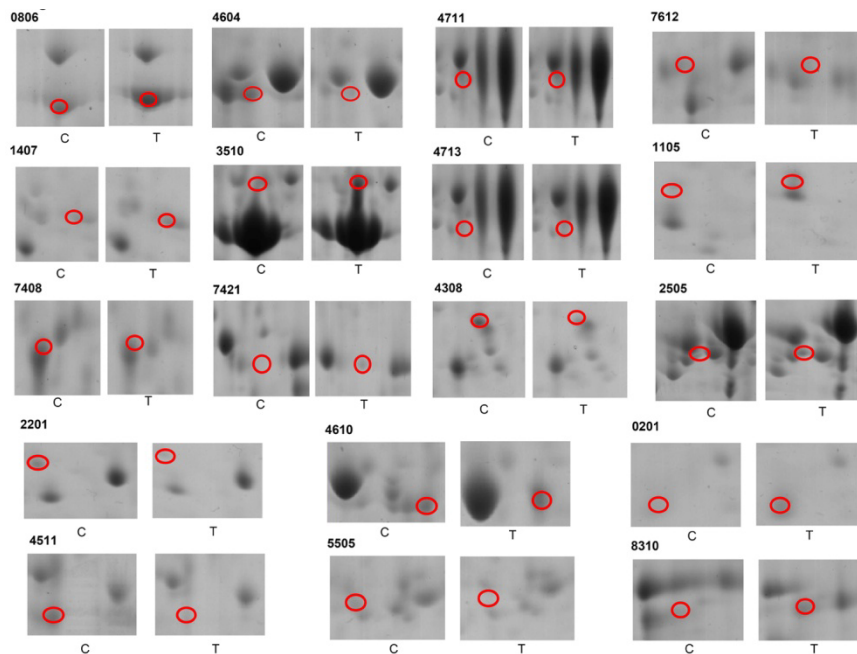


Fig. 3. Spots and spectra from MALDI-TOF MS/MS analysis of the trypsin digestion product of different spots. Peptide mixtures were loaded on the MALDI system, using the dried-droplet technique and α -cyano-4-hydroxycinnamic acid as matrix, and were analyzed using a 4700 Reflector spec #1 mass spectrometer.

Expression comparisons of each Coomassie brilliant blue-stained spot are shown in Fig. 2 and 3. Eighteen protein spots whose expression differed between the two groups were apparent. Of these, the expression of eight proteins was associated with the presence of ascorbic acid, with significant differences ($p < 0.05$); sixteen proteins were over-expressed and two proteins (capping protein (actin filament), gelsolin-1 and glutamate dehydrogenase 1) were down-regulated (Tab. 2).

Verification of differentially expressed proteins

The differentially expressed proteins were chosen for validation by quantitative real-time PCR analysis using RNA isolated from the tumor tissue. The genes encoding for differentially expressed proteins were calculated using the comparative threshold cycle (Ct) method after normalization to a control housekeeping gene for ribosomal RNA S18. Twelve proteins from the tissue with ascorbate treatment showed an increase in RNA expression, in comparison with the untreated control tissue (Fig. 4). The expression changes of most proteins were consistent with 2-DE results as shown in Fig. 3. However, capping protein (Capg) was not significantly up-regulated in tumor tissues of ascorbic acid-treated mice compared with control group mice.

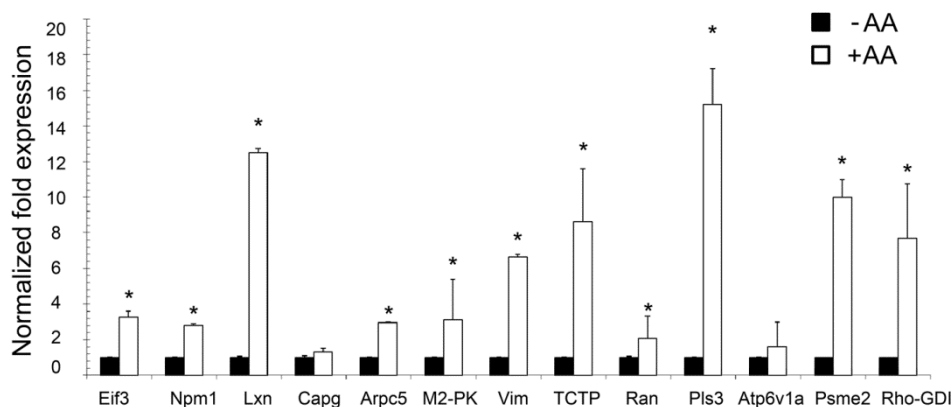


Fig. 4. RT-PCR analysis of mRNA levels in tumor tissues. Each mRNA level was normalized to 18s RNA level. Each data point represents a mean of three individual values and standard deviations. Quantitative analysis was performed and results are expressed as activity relative to untreated control group. Asterisks indicate statistically significant difference between treatment and untreated control condition ($*p < 0.01$). Abbreviations: Eif3 – Eukaryotic translation initiation factor 3 subunit 1; Npm1 – Nucleophosmin 1; Lxn – Latexin; Capg – Capping protein (actin filament), gelsolin-like; Arpc5 – Actin-related protein 2/3 complex subunit 5; M2-PK – M2-type pyruvate kinase; Vim – Vimentin; TCTP – Tumor protein, translationally-controlled 1; Ran – RAN, member RAS oncogene family; Pls3 – Plastin 3 precursor; Atp6v1a – ATPase, H⁺ transporting, lysosomal V1 subunit A; Psme2 – Proteasome activator complex subunit 2; Rho-GDI – Rho, GDP dissociation inhibitor β .

The effect of ascorbic acid on actin cytoskeleton

Among the proteins that were differentially regulated by ascorbic acid, actin, capping protein, actin-related protein and vimentin were cytoskeletal protein. Herein, we investigated whether ascorbic acid is able to affect the actin cytoskeleton in tumor nodules. Positivity to anti-mouse actin was seen in the middle and inner layer of a tissue. Reactive parts of the tissue were stained intensively brown as shown in Fig. 5. Immunohistochemistry of the tumor tissue section revealed that more actin distribution stained as brown was observed in the extracellular matrix of a tumor tissue treated with ascorbic acid than in the control (Fig. 5). However, vimentin showed no significant differences between tumor tissue treated with ascorbic acid and the control (data not shown).

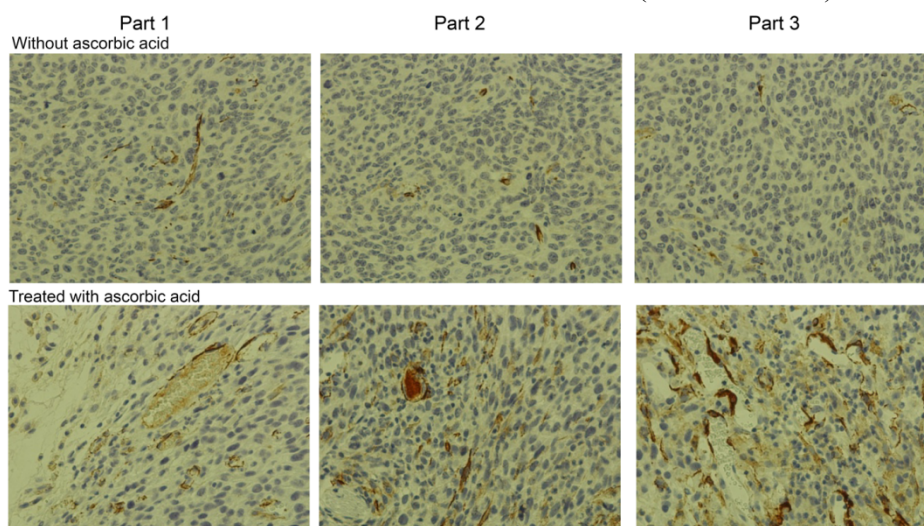


Fig. 5. Histological aspects of tumor tissue. The magnification views (200x) of tissues show cell body and extracellular matrix with actin cytoskeleton (brown staining). Actin cytoskeleton represented as brown staining was more abundant in tumor tissue treated with ascorbic acid than in control.

DISCUSSION

Detailed microscopic examination of the main organs as well as the lungs and local lymph nodes (other tissues known to harbor metastases from this tumor) have revealed a distinct inhibitory effect of oral vitamin treatment on the development of metastases [16]. Also, ascorbate supplementation augments the growth-inhibitory effect of dietary tyrosine and phenylalanine restriction on both primary and metastatic tumor growth, indicating an important adjuvant role [15]. Similarly, in Ehrlich ascites tumors, ascorbate reduces invasion and the tumors are characterized by long regions of basement membrane in the connective tissue stroma [25].

The mechanism of the action of ascorbic acid on tumor mass formation is unknown. The aim of the present study was to identify molecular changes not in recipient tissues of mouse but in tumor nodule coincident with susceptibility to ascorbic acid.

The proteomic approach was employed to screen a number of proteins that were differentially regulated by ascorbic acid treatment. Among the implicated proteins were metabolic proteins including M2-type pyruvate kinase, glutamate dehydrogenase 1, ATP synthase, ATPase, glyceraldehyde-3-phosphate dehydrogenase and alpha-enolase.

Ascorbic acid affected the distribution of cytoskeleton proteins in our study, suggesting a possibility that the tumor formation is associated with changes in the cytoskeleton array. There was an evident increase of actin protein following the treatment with ascorbic acid in two-dimensional electrophoresis data. In addition, although there was an evident decrease of capping protein following the treatment with ascorbic acid in two-dimensional electrophoresis data, there was no significant difference in mRNA level of capping protein. Also, immunohistochemistry revealed a more abundant distribution of actin in the cytoskeleton of the tumor tissue treated with ascorbic acid than in the control. Altogether, it seems that ascorbic acid affects remodeling rather than altering the expression of cytoskeleton proteins in tumor nodules.

In numerous experimental settings and biological systems, it has been established that translationally controlled tumor protein (TCTP) levels are highly regulated in response to a wide range of extracellular signals and cellular conditions [26]. Typically, growth signals [27] and cytokines [28, 29] have been reported to rapidly induce TCTP synthesis. The rapid adaptation of TCTP protein levels to alterations in cellular conditions implies that both synthesis and degradation are highly regulated [26]. There is plenty of evidence demonstrating that TCTP synthesis is regulated at both the transcriptional and the translational level. A study on about 50 human tissues [30] and other investigations on TCTP mRNA levels demonstrated that the expression of this protein is transcriptionally regulated [27]. The first molecular function of TCTP to be reported was calcium-binding activity [27]. It was shown that in mammalian cells, part of TCTP is bound to microtubules during most of the cell cycle, inclusive of the metaphase spindle, but is detached from the spindle after metaphase [31]. TCTP is phosphorylated by the protein kinase Plk [32], which is likely to cause detachment of TCTP from the mitotic spindle. Other molecular interactions of TCTP published to date include self-interaction [33]. As TCTP levels are considerably up-regulated during entry of cells into the cell cycle, the protein is believed to be important for cell growth and division. Overexpression of TCTP in mammalian cells resulted in slow growth and a delay in cell cycle progression [31]. An increase in TCTP levels was reported to be associated with increased chemoresistance [34, 35]. Overexpression of mammalian TCTP results in microtubule stabilization and alteration of cell morphology [31]. Together with TCTP's similarity to chaperones [36] and its recent characterization as an anti-apoptotic protein [37], these observations suggest that TCTP generally exerts a cytoprotective function. TCTP is not a tumor-specific protein, although its expression levels tend to be higher in tumors, compared to the corresponding normal tissue [37, 38], although this is not a general rule [38].

Acknowledgement. This research was supported by a National Research Foundation of Korea Grant funded by the Korean Government (2009-0070935).

REFERENCES

1. Padayatty, S.J., Sun, H., Wang, Y., Riordan, H.D., Hewitt, S.M., Katz, A., Wesley, R.A. and Levine, M. Vitamin C pharmacokinetics: implications for oral and intravenous use. **Ann. Intern. Med.** 140 (2004) 533-537.
2. Bram, S., Froussard, P., Guichard, M., Jasmin, C., Augery, Y., Sinoussi-Barre, F. and Wray, W. Ascorbic acid preferential toxicity for malignant melanoma cells. **Nature** 284 (1980) 629-631.
3. Bruchelt, G., Baader, L., Reith, A.G., Holger, N.L., Gebhardt, S. and Niethammer, D. Rationale for the use of ascorbic acid in neuroblastoma therapy. **Human Neuroblastoma Newark: Harwood Academic Publishers** (1993) 34-40.
4. Fujinaga, S., Sakagami, H., Kuribayashi, N., Takayama, H., Amano, Y., Sakagami, T. and Takeda, M. Possible role of hydrogen peroxide in apoptosis induction by ascorbic acid in human myelogenous leukemic cell lines. **Showa University Journal of Medical Sciences** 6 (1994) 135-144.
5. De Laurenzi, V., Melino, G., Savini, I., Annicchiarico-Petruzzelli, M., Finazzi-Agro, A. and Avigliano, L. Cell death by oxidative stress and ascorbic acid regeneration in human neuroectodermal cell lines. **Eur. J. Cancer** 31A (1995) 463-466.
6. Park, C.H. Biological nature of the effect of ascorbic acids on the growth of human leukemic cells. **Cancer Res.** 45 (1985) 3969-3973.
7. Park, C.H., Kimler, B.F., Bodensteiner, D., Lynch, S.R. and Hassanein, R.S. In vitro growth modulation by L-ascorbic acid of colony-forming cells from bone marrow of patients with myelodysplastic syndromes. **Cancer Res.** 52 (1992) 4458-4466.
8. Park, S., Han, S.S., Park, C.H., Hahm, E.R., Lee, S.J., Park, H.K., Lee, S.H., Kim, W.S., Jung, C.W., Park, K., Riordan, H.D., Kimler, B.F., Kim, K. and Lee, J.H. L-Ascorbic acid induces apoptosis in acute myeloid leukemia cells via hydrogen peroxidemediated mechanisms. **Int. J. Biochem. Cell. Biol.** 36 (2004) 2180-2195.
9. Fidler, I.J. Critical determinants of cancer metastasis: rationale for therapy. **Cancer Chemother. Pharmacol.** 43 (1999) S3-S10.
10. Mignatti, P. and Rifkin, D.B. Biology and biochemistry of proteinases in tumor invasion. **Physiol. Rev.** 73 (1993) 161-195.
11. Rath, M. and Pauling, L. Plasmin-induced proteolysis and the role of apoprotein(a), lysine and synthetic analogs. **J. Orthomolecular Med.** 7 (1992) 17-23.
12. Roomi, M.W., Roomi, N.W., Ivanov, V., Kalinovsky, T., Niedzwiecki, A. and Rath, M. Modulation of N-methyl-N-nitrosourea induced mammary tumors

- in Sprague-Dawley rats by combination of lysine, proline, arginine, ascorbic acid and green tea extract. **Breast Cancer Res.** 7 (2005) R291-R295.
13. Kohn, E.C. Development and prevention of metastasis. **Anticancer Res.** 13 (1993) 2553-2559.
 14. Wybieralska, E., Koza, M., Sroka, J., Czyz, J. and Madeja, Z. Ascorbic acid inhibits the migration of Walker 256 carcinosarcoma cells. **Cell. Mol. Biol. Lett.** 13 (2008) 103-111.
 15. Meadows, G.G., Pierson, H.F. and Abdallah, R.M. Ascorbate in the treatment of experimental transplanted melanoma. **Am. J. Clin. Nutr.** 54 (1991) 1284S-1291S.
 16. Taper, H.S., Jamison, J.M., Gilloteaux, J., Summers, J.L. and Calderon, P.B. Inhibition of the development of metastases by dietary vitamin C:K3 combination. **Life Sci.** 75 (2004) 955-967.
 17. Taper, H.S., Jamison, J.M., Gilloteaux, J., Gwin, C.A., Gordon, T., and Summers, J.L. In vivo reactivation of DNases in implanted human prostate tumors after administration of a vitamin C/K3. **J. Histochem. Cytochem.** 49 (2001) 109-119.
 18. Skalli, O., Ropraz, P., Trzeciak, A., Benzouana, G., Gillessen, D. and Gabbiani, G. A monoclonal antibody against α -smooth muscle actin: A new probe for smooth muscle differentiation. **J. Cell Biol.** 103 (1986) 2787-2796.
 19. Van Muijen, G.N.P., Ruiter, D.J. and Warnaar, S.O. Coexpression of intermediate filament polypeptides in human fetal and adult tissues. **Lab. Invest.** 57 (1987) 359-369.
 20. Goddard, M.J., Wilson, B. and Grant, J.W. Comparison of commercially available cytokeratin antibodies in normal and neoplastic adult epithelial and non-epithelial tissues. **J. Clin. Pathol.** 44 (1991) 660-663.
 21. Kobayashi, N. and Mundel, P. A role of microtubules during the formation of cell processes in neuronal and non-neuronal cells. **Cell Tissue Res.** 91 (1998) 163-174.
 22. Duncan, J.E. and Warrior, R. The cytoplasmic dynein and kinesin motors have interdependent roles in patterning the Drosophila oocyte. **Curr. Biol.** 12 (2002) 1982-1991.
 23. Lechner, A., Leech, C.A., Abraham, E.J., Nolan, A.L. and Habener, J.F. Nestin-positive progenitor cells derived from adult human pancreatic islets of Langerhans contain side population (SP) cells defined by expression of the ABCG2 (BCRP1) ATP-binding cassette transporter. **Biochem. Biophys. Res. Commun.** 293 (2002) 670-674.
 24. Yang, S.H., Kim, J.S., Oh, T.J., Kim, M.S., Lee, S.W., Woo, S.K., Cho, H.S., Choi, Y.H., Kim, Y.H., Rha, S.Y., Chung, H.C. and An, S.W. Genome-scale analysis of resveratrol-induced gene expression profile in human ovarian cancer cells using a cDNA microarray. **Int. J. Oncol.** 22 (2003) 741-750.
 25. Gruber, H.E., Tewfik, H.H. and Tewfik, F.A. Cytoarchitecture of Ehrlich ascites carcinoma implanted in the hind limb of ascorbic acid-supplemented mice. **Eur. J. Cancer.** 16 (1980) 441-448.

26. Bommer, U.A. and Thiele, B.J. The translationally controlled tumor protein (TCTP). **Int. J. Biochem. Cell. Biol.** 36 (2004) 379-385.
27. Bommer, U.A., Borovjagin, A.V., Greagg, M.A., Jeffrey, I.W., Russell, P., Laing, K.G., Lee, M. and Clemens, M.J. The mRNA of the translationally controlled tumor protein P23/TCTP is a highly structured RNA, which activates the dsRNA-dependent protein kinase PKR. **RNA** 8 (2002) 478-496.
28. Nielsen, H.V., Johnsen, A.H., Sanchez, J.C., Hochstrasser, D.F. and Schlotz, P.O. Identification of a basophil leukocyte interleukin-3-regulated protein that is identical to IgE-dependent histamine-releasing factor. **Allergy** 53 (1998) 642-652.
29. Teshima, S., Rokutan, K., Nikawa, T. and Kishi, K. Macrophage colony-stimulating factor stimulates synthesis and secretion of a mouse homolog of a human IgE-dependent histamine-releasing factor by macrophages in vitro and in vivo. **J. Immunol.** 161 (1998) 6356-6366.
30. Thiele, H., Berger, M., Skalweit, A. and Thiele, B.J. Expression of the gene and processed pseudogenes encoding the human and rabbit translationally controlled tumor protein (TCTP). **Eur. J. Biochem.** 267 (2000) 5473-5481.
31. Gachet, Y., Tournier, S., Lee, M., Lazaris-Karatzas, A., Poulton, T. and Bommer, U.A. The growth-related, translationally controlled protein P23 has properties of a tubulin binding protein and associates transiently with microtubules during the cell cycle. **J. Cell. Sci.** 112 (1999) 1257-1271.
32. Yarm, F.R. Plk phosphorylation regulates the microtubule-stabilizing protein TCTP. **Mol. Cell. Biol.** 22 (2002) 6209-6221.
33. Yoon, T., Jung, J., Kim, M., Lee, K.M., Choi, E.C. and Lee, K. Identification of the self-interaction of rat TCTP/IgE-dependent histamine-releasing factor using yeast two-hybrid system. **Arch. Biochem. Biophys.** 384 (2000) 379-382.
34. Sinha, P., Kohl, S., Fischer, J., Hütter, G., Kern, M., Köttgen, E., Dietel, M., Lage, H., Schnölzer, M. and Schadendorf, D. Identification of novel proteins associated with the development of chemoresistance in malignant melanoma using two-dimensional electrophoresis. **Electrophoresis** 21 (2000) 3048-3057.
35. Walker, D.J., Pitsch, J.L., Peng, M.M., Robinson, B.L., Peters, W., Bhisutthibhan, J. and Meshnick, S.R. Mechanisms of artemisinin resistance in the rodent malaria pathogen *Plasmodium yoelii*. **Antimicrob. Agents Chemother.** 44 (2000) 344-347.
36. Thaw, P., Baxter, N.J., Hounslow, A.M., Price, C., Waltho, J.P. and Craven, C.J. Structure of TCTP reveals unexpected relationship with guanine nucleotide-free chaperones. **Nat. Struct. Biol.** 8 (2001) 701-704.
37. Li, F., Zhang, D. and Fujise, K. Characterization of fortilin, a novel antiapoptotic protein. **J. Biol. Chem.** 276 (2001) 47542-47549.
38. Tuynder, M., Susini, L., Prieur, S., Besse, S., Fiucci, G., Amson, R. and Telerman, A. Biological models and genes of tumor reversion: Cellular reprogramming through tpt1/TCTP and SIAH-1. **Proc. Natl. Acad. Sci. USA** 99 (2002) 14976-14981.